



OPEN Molecular hydrogen as a potential mediator of the antitumor effect of inulin consumption

Victor Pascal-Moussellard¹, Jean-Pierre Alcaraz¹, Stéphane Tanguy¹, Cordélia Salomez-Ihl^{1,2}, Philippe Cinquin^{1,2}, François Boucher^{1,3}✉ & Emilie Boucher¹

Inulin consumption and dihydrogen (H_2) administration both exert antitumor effects on preclinical models as well as in clinical trials. As H_2 is one of the major byproducts of inulin fermentation by bacterial species of the gut microbiota (GM), we hypothesized that H_2 could mediate the antitumor effects of inulin. To provide evidence in favor of this hypothesis, we first determined the pattern of H_2 -exposure to which mice are subjected after inulin administration and developed an inhaled hydrogen therapy (H_2 T) protocol replicating this pattern. We then compared the effects on circulating immunity of a two-week daily inulin gavage with those of the corresponding H_2 T. We also compared the effects of inulin supplementation to those of the corresponding H_2 T on implanted melanoma growth and infiltration by T lymphocytes. Inulin and H_2 T induced a similar increase in circulating $CD4^+$ and $CD8^+$ T cells. In addition, both treatments similarly inhibited melanoma tumor growth. These results support a mechanism by which the H_2 resulting from inulin fermentation by the GM diffuses across the intestinal barrier and stimulates the immunosurveillance responsible for the antitumor effect.

Keywords Inulin, Molecular hydrogen, Melanoma, Immunosurveillance

Cancer is currently the second leading cause of death in the world, and it is projected to increase over the next 25 years. A recently published estimate forecasts a 76.6% increase in the number of cancer cases worldwide by 2050, accompanied by an 89.7% increase in the number of cancer deaths¹. This highlights the urgent need to develop novel therapeutic approaches and adapt our daily habits to address this escalating issue.

According to the Hallmarks of Cancer², the immune system plays a major role in cancer progression. Indeed, during the immunosurveillance process, several immune cells such as conventional $\alpha\beta$ TcR⁺ $CD8^+$ and $CD4^+$, and $\gamma\delta$ TcR⁺ T lymphocytes act together and target cancer cells to prevent tumor formation³. As this mechanism is crucial in the prevention of cancer development, many therapeutic strategies, grouped under the generic name of immunotherapy, have been developed to boost the activity of the immune system and counteract tumor progression⁴. To date, immunotherapy has revolutionized cancer treatments and improved the prognosis of patients suffering from various cancers^{5–7}. However, these treatments can have serious inflammation-related side effects such as autoimmunity or cardiac complications⁸, and some patients remain non-responders. To further improve cancer prognosis, innovative methods of immune system stimulation are being explored. One of the promising strategies is the modulation of the gut microbiota (GM).

GM refers to the 10^{14} microorganisms present in the human digestive tract⁹. The presence of specific bacteria in the GM, such as *Bifidobacterium* or *Akkermansia muciniphila*, has been shown to promote immunosurveillance and potentiate the response to immunotherapies and chemotherapies^{10–13}. Therefore, strategies to modulate the microbiota and promote the growth of beneficial bacterial species are in development to improve the outcome of cancer patients. Among these strategies stands the use of prebiotics, substrates that selectively support the growth of beneficial microorganisms conferring health benefits¹⁴.

Inulin is a prebiotic which promotes the growth of *Bifidobacterium* in the GM^{15,16}. Our group and others have provided preclinical evidence demonstrating an antitumor effect of inulin. In this context, inulin supplementation was shown to inhibit tumor growth in mouse models of melanoma, fibrosarcoma and ectopic colorectal cancer^{16–18}. This antitumor effect arises from an increased immunosurveillance. Tumor infiltration of conventional $CD4^+$ and $CD8^+$ T lymphocytes¹⁸ but also of $\gamma\delta$ T cells¹⁶ was shown to be increased by inulin supplementation in mice. Moreover, these immune cells were more prone to inhibit tumor growth as

¹Univ. Grenoble Alpes, CNRS, UMR 5525, VetAgro Sup, Grenoble INP, TIMC, Grenoble 38000, France.

²Univ. Grenoble Alpes, CHU Grenoble Alpes, Inserm, Grenoble CIC1406, 38000, France. ³Bâtiment Jean Roget, Université Grenoble Alpes, TIMC UMR, 5525, Equipe PRETA, La Tronche 38700, France. ✉email: francois.boucher@univ-grenoble-alpes.fr

a higher proportion of them was producing interferon- γ (IFN- γ). Our group has also shown that $\gamma\delta$ T cells are essential for the antitumor effect of inulin since inhibition of their activation prevents the beneficial effects of the supplementation¹⁶. Similarly, we have demonstrated that the bacterial component of the GM is crucial for the immunostimulatory and antitumor effects of inulin as the use of broad-spectrum antibiotics abrogates them¹⁶. It has also been shown that inulin supplementation enhances blood circulating immunity¹⁸. In addition to its well-described antitumor effects, inulin can also exert negative effects in specific contexts such as the intestinal pathologies colitis and colorectal cancer¹⁹. For example, in a mouse model of dextran sulfate sodium (DSS)-induced colitis, inulin supplementation increased the severity of colonic inflammation as well as weight loss and bleeding²⁰. Another study in mice, using DSS coupled with azoxymethane (AOM), showed that inulin supplementation not only aggravated inflammation but also promoted the development of colorectal tumors²¹. Finally, a study on mice spontaneously developing colorectal cancer independently of any inflammatory process, has shown that inulin supplementation increases tumor growth²². Altogether, these data suggest that inulin supplementation could be a satisfactory solution for the treatment of cancer patients. This excludes patients with intestinal cancers or with associated intestinal pathologies. Finally, to overcome the obstacle linked to the deleterious effects of inulin, one solution could be to directly administer the mediator of the antitumor effect of inulin.

Currently, the molecular and cellular mechanisms underlying the stimulation of immunity and the antitumor effect of inulin remain to be elucidated. It is hypothesized that it would result from metabolites and/or other elements produced by the microbiota upon inulin fermentation²³. The most popular candidates at present are 3 short-chain fatty acids (SCFAs), acetate, propionate and butyrate, which production is enhanced after inulin ingestion²⁴. Moreover, the abundance of bacterial species producing SCFAs was shown to correlate with reduced tumor size obtained by an inulin supplementation¹⁸. However, other compounds are produced during inulin fermentation. Molecular hydrogen (H_2) is one of them and is particularly promising because of its many biological effects. These are beginning to be well described but remain little known and incompletely understood. H_2 is the most abundant gas in the intestinal tract, and its daily production by the GM can reach up to 1 L in healthy human subjects under normal diet²⁵. Colonic H_2 production can be increased by enriching the diet with fibers and our group has established that *ad-libitum* inulin supplementation in mice transiently stimulates H_2 production during the post-prandial period²⁶.

Increased H_2 production by the GM could account for the antitumor effects of inulin supplementation. Beyond its antioxidant and anti-inflammatory properties extensively described in the literature²⁷, H_2 has also shown potential benefits in the context of cancer^{28,29}. The antitumor effect of H_2 seems to emerge from its ability to improve the immune system³⁰. For example, in patients with non-small cell lung cancer, H_2 inhalation increased the number of cytotoxic T cells and $\gamma\delta$ T cells in the blood, while reducing the exhaustion of circulating cytotoxic T cells^{31,32}. Similarly, H_2 restores exhausted CD8⁺ T cells in the blood of patients with colorectal cancer³³. Besides, a limited number of publications attributed a therapeutic role to H_2 produced by the GM. In a preclinical study on cardiac ischemia-reperfusion (IR) injury, suppression of the microbiota by antibiotic therapy led to an increased infarct size. This observation was interpreted as being due to the suppression of endogenous H_2 production by the GM³⁴. In addition, other studies have shown the protective effects of fructo-oligosaccharides (FOS) such as inulin on hepatic and cerebral IR. Here again, this was attributed to H_2 produced by intestinal FOS fermentation^{35–37}. In the light of these findings, it appears that enhancing H_2 endogenous production by the GM could have major protective effects in various pathophysiological situations. However, to our knowledge, the possible link between the immunostimulant antitumor effect of inulin and H_2 has never been explored.

Inulin and H_2 both exhibit antitumor effects through the activation and stimulation of the immune system. Since inulin ingestion increases H_2 production²⁶, we hypothesize that H_2 might be the mediator of inulin antitumor effect. The ideal approach to confirm this hypothesis would be to specifically block H_2 production by the microbiota after inulin administration and show the disappearance of the antitumor effect. Unfortunately, such strategy is not experimentally feasible without suppressing the other metabolites produced by inulin which would render the observations inconclusive. Therefore, we have chosen to provide indirect evidence by comparing the immune-antitumor signatures of inulin supplementation and H_2 -therapy (H_2 T). In this way, we have first characterized the H_2 production induced by inulin ingestion in mice. Based on these results, we were then able to develop a H_2 T that reproduced H_2 exposure of mice supplemented with inulin. Finally, we have compared the effects of inulin with those of H_2 T on circulating immunity and in a murine model of melanoma.

Results

Inulin gavage transiently stimulates GM H_2 production

To determine the production pattern of H_2 following inulin ingestion, two batches of 6 mice were force-fed with either water or inulin (70 mg in 150 μ L) at time point T = 0 (9:00 am). The 6 mice were then placed together in a preclinical device developed by our laboratory, to monitor their combined exhaled H_2 . Each measurement lasted 15 min to allow a sufficiently resolute determination of the HPR of the mice after gavage with water or inulin (Fig. 1a).

One hour after inulin ingestion, a rise in HPR was observed, which was almost twice as high as the basal HPR of the control group at the same time. HPR in the inulin group further increased, reaching a maximum production rate of 3.7 ± 0.8 nmol/s 2 h after inulin gavage (Fig. 1b). Therefore, inulin gavage induced a transient peak of H_2 production for at least 2 h. Although HPR decreased after 3 h, it remained significantly higher than the basal production of the control group. Indeed, 4 h after inulin gavage, the HPR of the inulin group was maintained at twice the value of the control group. Based on the production pattern observed after inulin gavage, we decided to expose the animals to 2 h of H_2 T, which corresponds to the peak of H_2 production induced by a 70 mg inulin gavage.

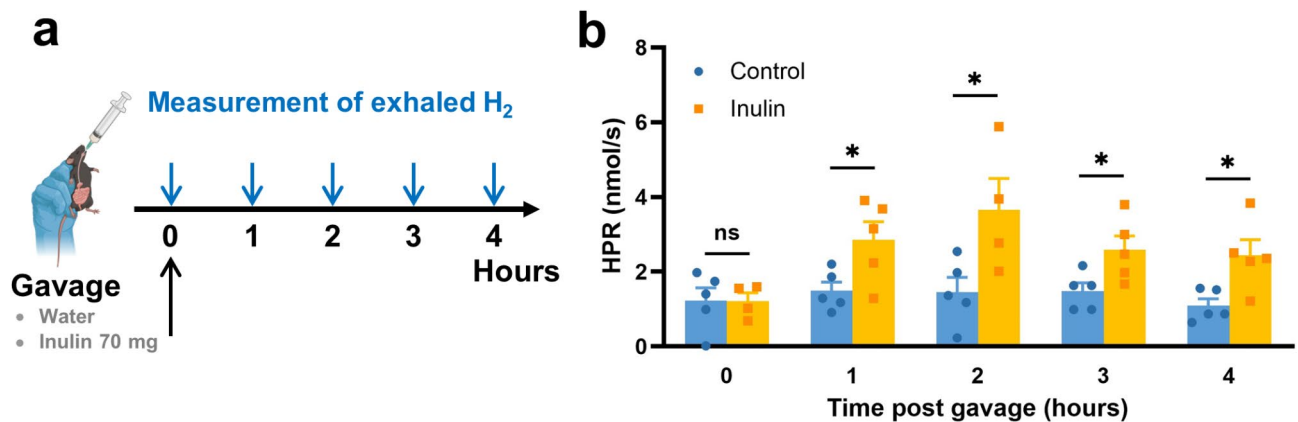


Fig. 1. Inulin ingestion induces a peak of H_2 production.

(a) Experimental schedule. C57BL/6 mice were force-fed with either 70 mg of inulin or water ($n=6$ mice per group) and exhaled H_2 production was measured at $T=0, 1, 2, 3$ and 4 h. Measures were repeated on 5 different days. (b) The production of exhaled H_2 was measured at different time points after the gavage, according to (a). Means \pm SEM of 4 to 5 independent HPR measurements, each performed on a group of 6 mice. HPR: Hydrogen Production Rate. * $p < 0.05$; Mann-Whitney test.

Inulin supplementation and H_2 T induce similar immunostimulatory effects in the blood

To compare the immunostimulatory effect of inulin to that of H_2 T, mice were either force-fed with 70 mg of inulin or exposed to 3% H_2 for 2 h, 5 times a week for 2 weeks. After 15 days, blood samples were collected from these mice, and their circulating immunity was analyzed using flow cytometry (Fig. 2a). Inulin increased the levels of circulating T lymphocytes (Fig. 2b). Additionally, both treatments similarly increased levels of circulating $CD8^+$ and $CD4^+$ T cells (Fig. 2c). Although both inulin supplementation and H_2 T slightly increased the frequency of circulating $\gamma\delta$ T cells, this was not statistically significant (Fig. 2c). The ability of these circulating lymphocytes to secrete IFN- γ was assessed by flow cytometry. The percentage of $CD4^+$, $CD8^+$ and $\gamma\delta$ T cells producing IFN- γ was significantly increased by both inulin and H_2 T (Fig. 2d). Furthermore, no significant difference was observed between inulin and H_2 T groups in any of the variables presented on this figure, suggesting a common immunological signature for the two treatments. Of note, in flow cytometry analysis, Double Negative (DN) cells were not taken into account or analysed (Figure S2).

Inulin supplementation and H_2 T tend to induce similar antitumor effects

As shown in the previous paragraph, inulin and H_2 T appear to exert similar immunostimulatory effects in the blood of naive mice. In order to compare the antitumor potential of the two treatments, mice were treated for 2 weeks either by gavage with 70 mg inulin, or by exposure for 2 h a day to 3% H_2 five times a week (H_2 T). After 15 days, all mice were subcutaneously injected with B16 OVA melanoma cells. Tumor growth was monitored for 15 days while maintaining the daily inulin treatment or H_2 T (Fig. 3a).

Both H_2 T and inulin supplementation significantly reduced tumor growth (Fig. 3b and c). On day 13 after tumor inoculation, the control group had an average tumor volume of 151.4 ± 48.8 mm³, compared to 39.3 ± 11.9 mm³ in the inulin supplemented group and 56.4 ± 13.2 mm³ in the H_2 T group (Fig. 3b). There was no significant difference in tumor growth between the inulin and H_2 T groups.

To determine the role of immunity in these antitumor effects, the tumor infiltration of $CD8^+$, $CD4^+$ and $\gamma\delta$ T lymphocytes was analyzed by flow cytometry. Due to the small size of some tumors in both treatment groups, immune infiltration could not be analyzed in all samples, which made statistical analysis impossible. Despite the absence of statistical comparisons, our results indicate that both inulin and H_2 T tended to increase the proportion of IFN- γ producing $CD8^+$, $CD4^+$ and $\gamma\delta$ T cells in the tumor (Fig. 3d, e and f). These results suggest that inulin and H_2 exposure induce a similar antitumor effect through stimulation of immunosurveillance.

Discussion

Ingestion of inulin is widely recognized for its anticancer properties, associated with changes in GM and stimulation of immunity. However, the mechanism by which inulin consumption leads to a stimulation of the immune system has yet to be elucidated. Here we propose that the H_2 produced by the GM during inulin fermentation is the mediator or one of the mediators, of this effect. To support this hypothesis, we have developed an inhalation H_2 T protocol modelled on H_2 production in mice given inulin gavage. Both inulin and H_2 T similarly increased the circulation and activation of $CD4^+$, $CD8^+$ and $\gamma\delta$ T lymphocytes in the blood. Moreover, both treatments similarly inhibited melanoma tumor growth and promoted the activation of tumor-infiltrated lymphocytes.

The H_2 T inhalation protocol we developed in this study was designed on the basis of H_2 production observed in mice after inulin gavage. The high diffusibility of H_2 in tissues³⁸ led us to assume that H_2 produced by the microbiota can easily pass the intestinal barrier and, once in the bloodstream, be distributed throughout the

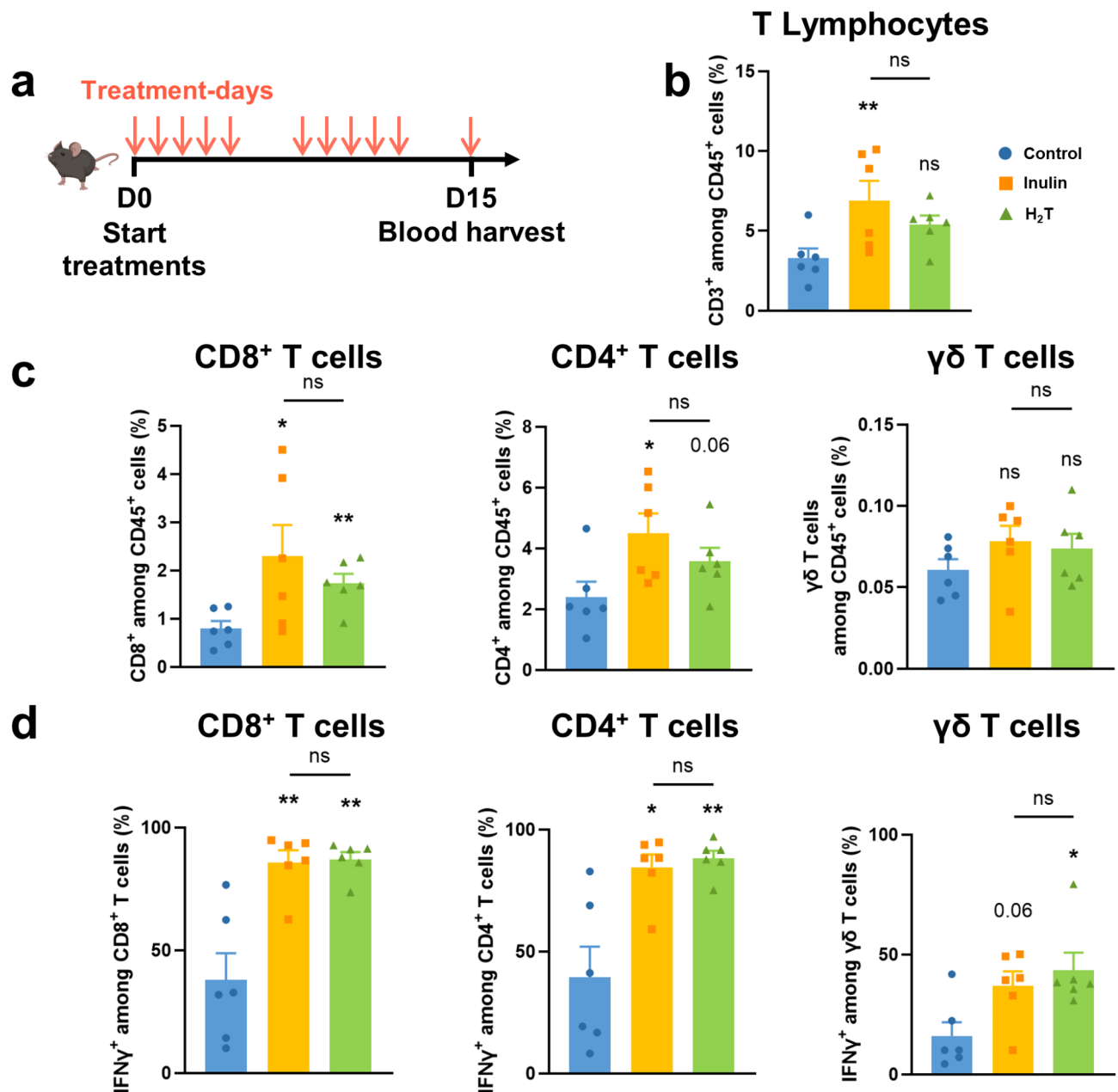


Fig. 2. Inulin gavage and H₂-therapy induce similar immunostimulant effects in the blood.

(a) Experimental timetable. C57BL/6 mice were either fed a standard diet (control, $n=6$), or force-fed with 70 mg of inulin (inulin, $n=6$), or treated with H₂-therapy for 2 hours (H₂T, $n=6$), 5 times a week. After 15 days of treatments, their blood was analyzed by flow cytometry. (b) Frequency of blood-circulating T lymphocytes, gated on CD45⁺, CD3⁺ cells of mice treated as described in (a). (c) Frequency of blood-circulating CD8⁺, CD4⁺ and γδ TcR⁺ T lymphocytes among all T lymphocytes, gated on CD45⁺ CD3⁺ cells of mice treated as described in (a). (d) Frequency of IFN-γ-producing CD8⁺, CD4⁺ and γδ TcR⁺ T lymphocytes of mice treated as described in (a). Means ± SEM. * $p < 0.05$ vs. control; ** $p < 0.01$ vs. control; ns: non-significant; Mann-Whitney test.

body. In addition, both *per os* administration of H₂-rich water and inhalation of H₂ lead to similar concentrations of H₂ in arterial blood³⁹. Therefore, it can be reasonably considered that the two treatments used in this study led to similar H₂ exposures.

Previous work by our group has demonstrated that inulin exerts an antitumor effect in mice, not only on melanoma but also on fibrosarcoma and colorectal cancer¹⁶. Similarly, H₂ has been shown to be effective in the treatment of colorectal cancer both on cell cultures and on xenograft mouse models⁴⁰. Inhalation of H₂ has also been shown to increase Progression Free-Survival (PFS) in patients with stage IV colorectal carcinoma by alleviating the exhaustion of CD8⁺ T lymphocytes³³. In addition, in a mouse model of fibrosarcoma, tumor growth was inhibited by an innovative H₂-treatment consisting of intratumoral implantation of magnesium

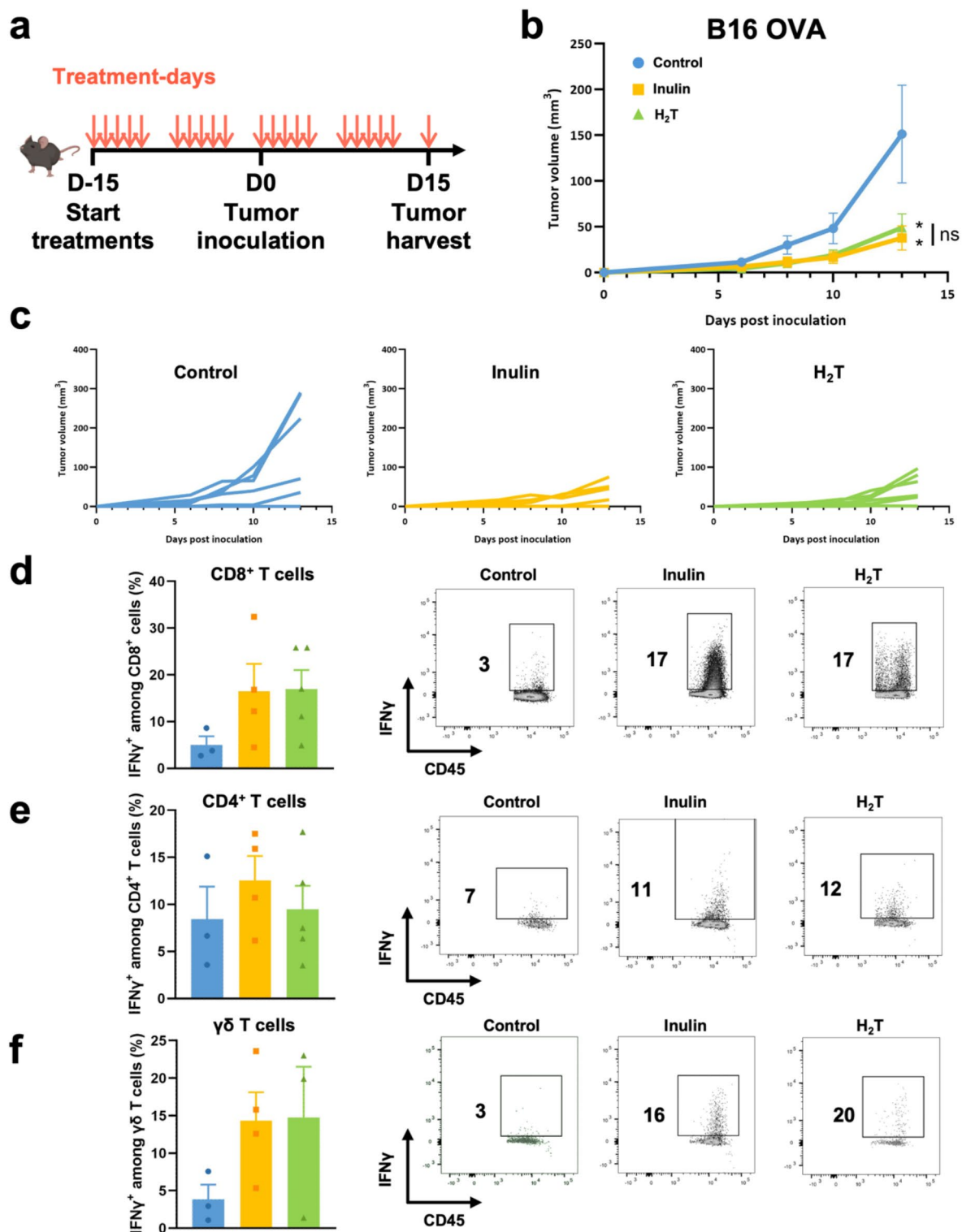


Fig. 3. Inulin gavage and H₂T-therapy tend to induce similar antitumor effects.

(a) Experimental timetable. C57BL/6 mice were either fed a standard diet (control, $n=6$), or force-fed with 70 mg of inulin (inulin, $n=6$), or treated with H₂T-therapy for 2 h (H₂T, $n=6$), 5 times a week. After 15 days of treatments, 2×10^5 B16 OVA melanoma cells were subcutaneously injected in the right flank of each mouse. (b–c) Tumor growth of mice treated as described in (a), represented as means \pm SEM (b) or individual growths (c). (d–f) Frequency of B16 OVA tumor-infiltrated IFN- γ -producing cells gated on CD45⁺ CD3⁺ (d) CD8⁺ (e) CD4⁺ or (f) $\gamma\delta$ TcR⁺, from mice treated as in (a). Means \pm SEM ($n=3-6$). * $p < 0.05$ vs. control; Two-Way ANOVA test and Mann-Whitney test.

rods coated with calcium carbonate nanoparticles generating H_2 directly in the tumor microenvironment. The antitumor effect observed was accompanied by an infiltration of $CD4^+$ and $CD8^+$ T cells in the tumor⁴¹. These studies suggest that H_2 induces similar effects in fibrosarcoma and colorectal cancer to those observed in melanoma in this study. Thus, H_2 may be responsible for the anticancer properties of inulin.

The benefits of H_2 for cancer treatment is well established. However, its mode of action remains unclear. Some studies suggest that H_2 acts directly on cancer cells through specific cellular pathways⁴². Other works indicate that its anticancer effect is mediated through immune modulation. In several mouse cancer models, H_2 treatments have been shown to increase the infiltration of $CD4^+$ and $CD8^+$ T lymphocytes in the tumor and enhance T_H1 -polarized T lymphocytes^{41,43}. Clinical studies have shown that H_2 , whether administered alone or in combination with other treatments, helps restoring $CD8^+$ T cell exhaustion^{30,33,44}. Additionally, the combination of H_2 inhalation and immunotherapy has shown a synergistic effect in lung cancer patients³². All these studies support the involvement of the immune system in the antitumor effect of H_2 . This aligns with our findings, which show that both inulin and H_2 T induce comparable immunosurveillance profiles in the blood and tumors. H_2 production from inulin fermentation may therefore activate the immune system and inhibit tumor growth.

The stimulation of the immune system induced by H_2 administration may seem incompatible with its widely described anti-inflammatory effect. Indeed, studies on various animal models with acute or chronic inflammation have shown that H_2 T allows to alleviate the levels of tissue $TNF-\alpha$, IL-6 and IL-17^{45–47}. Moreover, clinical and pre-clinical studies have shown that H_2 T also reduces C-reactive protein (CRP) levels in the blood of rats after lung IR⁴⁸ but also in the blood of patients with different inflammatory pathologies such as rheumatoid arthritis or rheumatic polymyalgia^{49,50}. More intriguingly, H_2 T was shown to reduce the number of T lymphocytes producing IFN- γ in non-infectious conditions like pregnancy⁵¹ or allografts⁵². This is contradictory with our findings on healthy mice and in cancer situations⁴³. In general terms, it appears that H_2 exerts anti-inflammatory effects in over-inflammatory conditions whereas in physiological or cancer contexts it promotes an activation of the immune system towards a T_H1 -polarized response.

This study aims at highlighting the link between the antitumor and immunostimulatory effects of inulin and H_2 . However, the mechanism underlying this relationship remains unknown. Previous studies from our group have suggested that the effects of inulin treatment depend on $\gamma\delta$ TcR activation¹⁶. $\gamma\delta$ TcR can recognize a wide range of molecules and be activated by Major Histocompatibility Complex (MHC) molecules (class I and II), MHC-like molecules, phosphoantigens presented by butyrophilins, and unbound antigens^{53,54}. Notably, antigen recognition is not mandatory for $\gamma\delta$ TcR activation, conformational changes in MHC or butyrophilin molecules alone may be sufficient⁵⁵. We propose that H_2 produced through inulin fermentation may induce such conformational changes, leading to $\gamma\delta$ T cell activation. Further in vitro experiments are needed to elucidate the mechanisms involved and determine the role of H_2 in this process. Furthermore, other immune cell populations may contribute to the observed effects of inulin and H_2 . In the present study, flow cytometry analysis did not account for NKT cells, regulatory T cells (Tregs) and DN T cells, which collectively constitute up to 5% of circulating immune cells in mice⁵⁶. Additionally, epigenetic regulation of the *Ifng* gene may play a role. This gene can be epigenetically silenced through H3K27 methylation^{57,58}, and H_2 has been shown to decrease this methylation via H3K27 demethylase induction⁵⁹. Therefore, analyzing the H3K27 methylation status of *Ifng* in circulating and infiltrated $CD4^+$, $CD8^+$, and $\gamma\delta$ T cells could provide insight into how H_2 produced from inulin ingestion stimulates IFN- γ production. Both hypotheses are not mutually exclusive and may act synergistically in mediating the antitumor effects of inulin. However, these two last hypotheses have not yet been experimentally validated. Investigating them is essential to elucidate the mechanisms underlying the antitumor effect of inulin.

As previously mentioned, bacterial fermentation of inulin produces various metabolites. This study focuses on the role of H_2 , though other metabolites may also interact with H_2 to enhance antitumor immunity. Short-chain fatty acids (SCFAs), well-known byproducts of inulin fermentation, have been linked to reduced tumor size¹⁸. Additionally, SCFAs support T_H1 polarization of T cells⁶⁰, as observed in our study. Among SCFAs, butyrate has been recognized for its antitumor properties⁶¹. Notably, bacterial H_2 production has been shown to stimulate butyrate production within the same environment⁶², suggesting that inulin may enhance butyrate secretion via increased H_2 levels. In turn, butyrate could mediate immune stimulation and contribute to tumor growth inhibition. However, the role of SCFAs in cancer remains uncertain. While preclinical studies indicate that SCFAs can inhibit tumor progression through $CD8^+$ T cell activation⁶¹, their influence on cancer treatment is still a matter of debate⁶³. Some studies report that elevated blood levels of butyrate and propionate correlate with resistance to anti-CTLA-4 immunotherapy and an increased proportion of circulating Tregs⁶⁴. Additionally, in vivo administration of butyrate has been shown to counteract the antitumor effects of radiotherapy and vancomycin in mice with B16 melanoma⁶⁵. Overall, existing literature suggests a potential role for SCFAs in the antitumor effects of inulin. However, conflicting findings highlight the complexity of their impact in cancer contexts.

Despite the convincing results presented in this paper, we are aware of the limitations of our study. A complete demonstration of H_2 as the mediator of the antitumor effect of inulin would require to either prevent H_2 production by the microbiota or to specifically and totally trap H_2 produced through inulin fermentation. We have already shown that the antitumor effect of inulin is completely abrogated when the microbiota is depleted by large spectrum antibiotics¹⁶. Nevertheless, many metabolites and byproducts other than H_2 are produced by the fermentation of inulin through the GM²³. Therefore, even a specific inhibition or invalidation of the dehydrogenases responsible of bacterial H_2 production would have consequences for other inulin catabolites and would render the results inconclusive. In addition to the impossibility of specifically trapping the H_2 produced by the intestinal fermentation of inulin, a methodological difficulty arose in our study which was directly linked to the antitumor efficacy of the treatments. In the groups that received either inulin or H_2 T, mice developed very small tumors, i.e. around 39.3 and 56.4 mm³. In addition, two animals died in the control group due to the

tumor model (major intestinal metastases observed at necropsy) and their tumor-infiltrated immunity could not be analyzed. As a result, small amounts of biological material were collected, leading to a limited number of infiltrated lymphocytes labeled for flow-cytometry analysis. This low number of cells was not analyzable, and the corresponding samples had to be discarded from our study. Thus, group size was restricted to $n=3$ instead of $n=6$, which explains the absence of significant differences between groups for the analysis of the infiltrated immunity. Furthermore, in the treated groups, a high degree of variability was observed, with some animals not responding at all to the treatments. This variability obviously had an impact on statistical comparisons. In summary, final groups size and inter-individual variability explain the absence of statistical comparison between experimental groups in the analysis of tumor infiltration. Further studies could address this question, as the sample size needed to detect statistical differences can now be determined based on the inter-individual variability demonstrated in this work.

It is generally admitted that inulin and non-digestible dietary fibers modulate the microbiota¹⁵, stimulate the immune system¹⁶, act synergistically with immunotherapies^{16,18}, and promote H_2 production by the GM²⁶. The results of this study suggest that H_2 produced through inulin fermentation by the GM could enter the bloodstream and stimulate T lymphocytes. Due to its high solubility, H_2 could also diffuse into surrounding tissues, such as the skin. Various immune cells, including $\gamma\delta$ T cells, are located within the skin and play a crucial role in immunosurveillance⁶⁶. Therefore, the enhanced immunosurveillance observed after two weeks of inulin supplementation or H_2 T could originate from the skin or any other tissue harboring resident $\gamma\delta$ T cells.

As regards the clinical applicability of these treatments, inulin supplementation has demonstrated no acute⁶⁷ or chronic⁶⁸ toxicity. Likewise, no cytotoxicity⁶⁹ or genotoxicity⁷⁰ has been observed for H_2 . However, inulin-type fiber supplementation may not be suitable for patients with certain conditions, such as colorectal cancer (CRC) or colitis. Studies have shown that a fiber-rich diet—particularly one high in inulin—can promote the development and growth of colon tumors in two similar mouse models. In the first, $Apc^{min/+}$ transgenic mice spontaneously developed colon tumors⁷¹, while in the second, $Apc^{min/+}$ transgenic mice were injected with azoxymethane to induce colorectal cancer⁷². In addition, inulin supplementation has been found to exacerbate colonic inflammation in a mouse model of dextran sodium sulfate (DSS)-induced colitis²⁰. In contrast, the effects of H_2 in these pathological conditions appear to be beneficial. Both H_2 inhalation⁴⁰ and H_2 -rich water supplementation⁷³ have been shown to inhibit tumor growth in a mouse colorectal cancer xenograft model. Moreover, H_2 has been found to suppress DSS-induced colonic inflammation in mice⁷⁴. A very limited number of clinical studies have evaluated the effects of H_2 treatments on cancer progression in humans. These studies have reported that H_2 -therapy prolongs progression-free survival in patients with colorectal³³ and non-small cell lung cancer patients^{31,32}, whether H_2 is given alone or in combination with immunotherapy or chemotherapy. In addition, one final clinical trial showed that H_2 limits cancer progression in 57.5% of patients with different types of advanced cancer (stages III and IV)⁷⁵. Given these findings, a potential alternative for patients who cannot tolerate inulin could be the direct administration of the mediators responsible for inulin's antitumor effects, offering a promising therapeutic strategy.

H_2 , the proposed mediator, can be administered in various ways such as inhalation⁷⁶ or ingestion of H_2 -rich water⁷⁷. For skin cancer applications, developing an H_2 -rich ointment could be a solution to directly enhance the immune response within the cutaneous tumor. These methods would offer personalized therapy tailored to each patient and his needs. They could also prevent side effects caused by conventional immunotherapy, chemotherapy, and radiotherapy⁷⁸.

Methods

Animals and inulin treatment

Female C57BL/6 mice (5 to 6 weeks old) were provided by Janvier Labs (Le Genest-Saint-Isle, France) and housed at "Plateforme de Haute Technologie Animale (PHTA)" UGA core facility (Grenoble, France), EU0197, Agreement #C38-51610006, under specific pathogen-free conditions, temperature-controlled environment with a 12 h/12 h light/dark cycle and had *ad libitum* access to water and standard food (Altromin LASQCdiet[®] Rod16). Animal housing and procedures were conducted in accordance with the recommendations of the Veterinary Services Department and the French Ministry of Research, in compliance with the European Directive 2010/63/EU and the recommendations for health monitoring promulgated by the Federation of European Laboratory Animal Science Associations. Protocols involving animals were reviewed by the local ethic committee "Comité d'Ethique pour l'Expérimentation Animale #12, ComEth-Grenoble" and approved by the Ministry of Research (APAFIS#39565-2022112413525573.v2). Mice in the inulin groups were force-fed with 70 mg of inulin (Inulin Orafit[®] GR, Beneo, Belgium) diluted in 150 μ L of water (450 g/L), 5 times a week. To ensure that the force-feeding did not introduce experimental bias, mice from the other groups were force-fed with 150 μ L of water at the same time points. All animals were euthanized by cervical dislocation at the end of the procedure or when they were excluded during follow-up because their tumor reached the size defined as the ethical limit. Finally, the authors confirm that the study is reported in accordance with ARRIVE guidelines.

Exhaled H_2 assessment

Mice were placed in a previously described preclinical device²⁶ allowing to follow H_2 production within a hermetic chamber in which environmental parameters (O_2 , CO_2 , humidity and temperature) are constantly controlled. The air contained in the chamber was continuously pumped by a ATO SKY 100 (0 to 100 ppm \pm 0.01) to analyze its H_2 content and reintroduced in the chamber (shunt flowrate = 375 mL/min). The H_2 production rate (HPR) was determined as previously described and expressed in nanomole of H_2 per second (nmol/s). Measurements were performed on batches of 6 mice, lasted for 15 min, and were repeated at T = 0 (9:00 am), 1, 2, 3 and 4 h after gavage with inulin or water. During each measure, mice did not have access to food and water. Between two measures, mice were returned to their usual housing with access to food and water.

H₂-therapy (H₂T)

H₂ was delivered through inhalation using an original device developed by the laboratory (Figure S1). This device allows to produce a gas mixture composed of 3% H₂, 76% N₂ and 21% O₂. A cylinder containing a N₂/H₂ mixture (96.4%/3.6%) was connected to a first flowmeter by polyurethane tubing. O₂ was produced by an O₂ concentrator Devilbliss[®] connected to a second flowmeter by polyurethane tubing. O₂ flow was mixed with the N₂/H₂ flow by connecting the two hoses downstream the flowmeters. The two flowmeters were adjusted to deliver the final gas mixture at 1.27 L/min directly into an airtight NexGen Mouse 500 (Allentown, USA) cage for ventilated racks, enabling the animals to be kept in their usual environment during H₂T. The gas outlet was provided by a hole in the lid to maintain the cage at atmospheric pressure. H₂T lasted for 2 h a day and was applied 5 times a week. The H₂ concentration in the cage was regularly controlled with a Quintron BreathTracker, using air samples taken from the cage during exposure to H₂.

Cell line

Ovalbumin-expressing B16 melanoma cells (B16-OVA) were kindly provided by C. Fournier, Inserm U1209. B16-OVA were cultured in a complete medium composed of 10% Fetal Bovine Serum (FBS) (Gibco) Dulbecco's modified Eagle's medium (DMEM) (Gibco) supplemented with 1% non-essential amino acids, 1 mM sodium pyruvate, 50 U/mL penicillin, and 50 µg/mL streptomycin (all from Gibco). For plasmid selection, geneticin selective antibiotic (500 µg/ml, Sigma) was added to the cultures. The cell line was tested as mycoplasma-free.

Tumor implantation

Mice received subcutaneous injection of 2×10^5 B16-OVA cells in 100 µL PBS in the right flank. Once palpable, tumors were measured daily using a caliper, and tumor volume was determined using the following formula: $V_{\text{tumor}} = 0.5 \times (\text{width} \times \text{length}^2)$. The maximal ethic tumor size was calculated as: width \times length = 150 mm².

Tumor digestion

Tumors were collected in complete Roswell Park Memorial Institute (RPMI) medium (Gibco), lacerated with scalpels, and digested with Liberase[™] 2.5 mg/mL (Roche). Finally, tumors were gently crushed through a 70 µm cell strainer, washed, and resuspended in 10% FBS complete RPMI.

Blood sample preparation

Blood was collected *via* retro-orbital sampling under Isoflurane anesthesia just prior to euthanasia. Samples were stored in K2E tubes (BD Medical). After centrifugation, blood pellets were resuspended in 1 mL Red Blood Cell Lysis buffer 1X (Sigma) and washed with 10% FBS complete RPMI.

Flow cytometry

To allow intracellular labelling of cytokines, cell suspensions were stimulated for 4 h at 37 °C with 50 ng/mL phorbol 12-myristate 13-acetate (PMA) (Sigma), 1 µg/mL ionomycin (Sigma), and Golgi Stop[™] (BD Biosciences). For extracellular labelling, cells were incubated with 200 ng of each antibody, and dead cells were labelled using Live/Dead[™] Fixable Yellow Dead Cell Stain kit for 405 nm excitation (Thermo Fischer Scientific). Antibodies were used to target extracellular proteins CD45 (30-F11), CD3 (17A2 or 145-2C11), CD4 (GK1.5), γδ-TcR (eBioGL3 (GL-3, GL3) (Biolegend and eBiosciences) (Table S1). To allow intracellular labelling, cells were first permeabilized using a FoxP3 staining buffer kit (eBioscience). Antibodies were used to target intracellular cytokine IFN-γ (XMG1.2) (Biolegend) (Table S1). After intracellular labelling, cells were fixed and stored using FACS Lysing Solution 1X (BD Biosciences). All data were collected using a BD Biosciences FACS Lyric and analyzed using FlowJo software. The gating strategy is detailed in Figure S2. Briefly, T cells were selected as CD45⁺ CD3⁺ cells. γδ T cells were selected as CD45⁺ CD3⁺ γδTcR⁺ cells. CD4⁺ T cells were selected as CD45⁺ CD3⁺ γδTcR[−] CD4⁺ cells. CD8⁺ T cells were selected as CD45⁺ CD3⁺ γδTcR[−] CD4[−] cells. This gating strategy neglected CD45⁺ CD3⁺ γδTcR[−] CD4[−] CD8[−], DN represent less than 1% of blood T lymphocytes in naive C57BL/6 mice⁷⁷. Other immune cells such as NKT and Tregs were also not considered in the analyses.

Statistical analysis

Data are presented as means ± SEM. Two-way ANOVA test was used to compare tumor growth. Significant outliers were determined by Grubb's test on the last day of tumor growth. Non-parametric Mann-Whitney tests were used to compare results of flow cytometry and *in vivo* HPR.

Data availability

Data are available from the corresponding author upon reasonable request.

Received: 30 December 2024; Accepted: 27 March 2025

Published online: 03 April 2025

References

1. Bizuayehu, H. M. et al. Global disparities of cancer and its projected burden in 2050. *JAMA Netw. Open.* **7** (11), e2443198. <https://doi.org/10.1001/jamanetworkopen.2024.43198> (2024).
2. Hanahan, D. & Weinberg, R. A. Hallmarks of cancer: the next generation. *Cell* **144** (5), 646–674. <https://doi.org/10.1016/j.cell.2011.02.013> (2011).
3. Dunn, G. P., Old, L. J. & Schreiber, R. D. The three Es of cancer immunoediting. *Annu. Rev. Immunol.* **22**, 329–360. <https://doi.org/10.1146/annurev.immunol.22.012703.104803> (2004).

4. Finn, O. J. A Believer's overview of cancer immunosurveillance and immunotherapy. *J. Immunol.* **200** (2), 385–391. <https://doi.org/10.4049/jimmunol.1701302> (2018).
5. Zhang, Y. & Zhang, Z. The history and advances in cancer immunotherapy: Understanding the characteristics of tumor-infiltrating immune cells and their therapeutic implications. *Cell. Mol. Immunol.* **17** (8), 807–821. <https://doi.org/10.1038/s41423-020-0488-6> (2020).
6. Gibney, G. T. & Atkins, M. B. Choice of first-line therapy in metastatic melanoma. *Cancer* **125** (5), 666–669. <https://doi.org/10.1002/cncr.31774> (2019).
7. Kim, S. Y. & Halmos, B. Choosing the best first-line therapy: NSCLC with no actionable oncogenic driver. *Lung Cancer Manag.* **9** (3), LMT36. <https://doi.org/10.2217/lmt-2020-0003> (2020).
8. Kroschinsky, F. et al. Intensive care in hematological and oncological patients (iCHOP) collaborative group. New drugs, new toxicities: severe side effects of modern targeted and immunotherapy of cancer and their management. *Crit. Care.* **21** (1), 89. <https://doi.org/10.1186/s13054-017-1678-1> (2017).
9. Thursby, E. & Juge, N. Introduction to the human gut microbiota. *Biochem. J.* **474** (11), 1823–1836. <https://doi.org/10.1042/BCJ20160510> (2017).
10. Sivan, A. et al. Commensal bifidobacterium promotes antitumor immunity and facilitates anti-PD-L1 efficacy. *Science* **350** (6264), 1084–1089. <https://doi.org/10.1126/science.aac4255> (2015).
11. Gopalakrishnan, V. et al. Gut Microbiome modulates response to anti-PD-1 immunotherapy in melanoma patients. *Science* **359** (6371), 97–103. <https://doi.org/10.1126/science.aan4236> (2018).
12. Zhang, M., Liu, J. & Xia, Q. Role of gut Microbiome in cancer immunotherapy: from predictive biomarker to therapeutic target. *Exp. Hematol. Oncol.* **12** (1), 84. <https://doi.org/10.1186/s40164-023-00442-x> (2023).
13. Viaud, S. et al. The intestinal microbiota modulates the anticancer immune effects of cyclophosphamide. *Science* **342** (6161), 971–976. <https://doi.org/10.1126/science.1240537> (2013).
14. Gibson, G. R. et al. Expert consensus document: the international scientific association for probiotics and prebiotics (ISAPP) consensus statement on the definition and scope of prebiotics. *Nat. Rev. Gastroenterol. Hepatol.* **14** (8), 491–502. <https://doi.org/10.1038/nrgastro.2017.75> (2017).
15. Vandeputte, D. et al. Prebiotic inulin-type Fructans induce specific changes in the human gut microbiota. *Gut* **66** (11), 1968–1974. <https://doi.org/10.1136/gutjnl-2016-313271> (2017).
16. Boucher, E. et al. Inulin prebiotic reinforces host cancer immunosurveillance via $\gamma\delta$ T cell activation. *Front. Immunol.* **14**, 1104224. <https://doi.org/10.3389/fimmu.2023.1104224> (2023).
17. Li, Y. et al. Prebiotic-Induced Anti-tumor immunity attenuates tumor growth. *Cell. Rep.* **30** (6), 1753–1766e6. <https://doi.org/10.1016/j.celrep.2020.01.035> (2020).
18. Han, K. et al. Generation of systemic antitumor immunity via the in situ modulation of the gut Microbiome by an orally administered inulin gel. *Nat. Biomed. Eng.* **5** (11), 1377–1388. <https://doi.org/10.1038/s41551-021-00749-2> (2021).
19. Olierio, M., Alaoui, A. A., McCartney, C. & Santos, M. M. Colorectal cancer and inulin supplementation: the good, the bad, and the unhelpful. *Gastroenterol. Rep. (Oxf)*. **12**, goae058. <https://doi.org/10.1093/gastro/goae058> (2024).
20. Miles, J. P. et al. Supplementation of low- and high-fat diets with fermentable fiber exacerbates severity of DSS-induced acute colitis. *Inflamm. Bowel Dis.* **23** (7), 1133–1143. <https://doi.org/10.1097/MIB.0000000000001155> (2017).
21. Tian, S. et al. Refined fiber inulin promotes inflammation-associated colon tumorigenesis by modulating microbial succinate production. *Cancer Rep. (Hoboken)*. **6** (11), e1863. <https://doi.org/10.1002/cnr.2.1863> (2023).
22. Misikangas, M. et al. Inulin results in increased levels of beta-catenin and Cyclin D1 as the adenomas increase in size from small to large in the min/++ mouse. *Br. J. Nutr.* **99** (5), 963–970. <https://doi.org/10.1017/S0007114507853414> (2008).
23. Sheng, W., Ji, G. & Zhang, L. Immunomodulatory effects of inulin and its intestinal metabolites. *Front. Immunol.* **14**, 1224092. <https://doi.org/10.3389/fimmu.2023.1224092> (2023).
24. Tarini, J. & Wolever, T. M. The fermentable fibre inulin increases postprandial serum short-chain fatty acids and reduces free-fatty acids and Ghrelin in healthy subjects. *Appl. Physiol. Nutr. Metab.* **35** (1), 9–16. <https://doi.org/10.1139/H09-119> (2010).
25. Mutuyemungu, E., Singh, M., Liu, S. & Rose, D. J. Intestinal gas production by the gut microbiota: a review. *J. Funct. Foods.* **100**, 105367. <https://doi.org/10.1016/j.jff.2022.105367> (2023).
26. Pascal-Moussellard, V. et al. An ethically guided preclinical device for phenotyping H_2 production in laboratory rodents. *Anim. Model. Exp. Med.* **7** (4), 553–561. <https://doi.org/10.1002/ame2.12460> (2024).
27. Artamonov, M. Y. et al. Molecular hydrogen: from molecular effects to stem cells management and tissue regeneration. *Antioxid. (Basel)*. **12** (3), 636. <https://doi.org/10.3390/antiox12030636> (2023).
28. Li, S. et al. Hydrogen gas in cancer treatment. *Front. Oncol.* **9**, 696. <https://doi.org/10.3389/fonc.2019.00696> (2019).
29. Mohd Noor, M. N. Z. et al. A systematic review of molecular hydrogen therapy in cancer management. *Asian Pac. J. Cancer Prev.* **24** (1), 37–47. <https://doi.org/10.31557/APJCP.2023.24.1.37> (2023).
30. Zhou, W., Zhang, J., Chen, W. & Miao, C. Prospects of molecular hydrogen in cancer prevention and treatment. *J. Cancer Res. Clin. Oncol.* **150** (4), 170. <https://doi.org/10.1007/s00432-024-05685-7> (2024).
31. Chen, J. B. et al. Two weeks of hydrogen inhalation can significantly reverse adaptive and innate immune system senescence patients with advanced non-small cell lung cancer: a self-controlled study. *Med. Gas Res.* **10** (4), 149–154. <https://doi.org/10.4103/2045-9912.304221> (2020).
32. Chen, J. B. et al. Hydrogen therapy can be used to control tumor progression and alleviate the adverse events of medications in patients with advanced non-small cell lung cancer. *Med. Gas Res.* **10** (2), 75–80. <https://doi.org/10.4103/2045-9912.285560> (2020).
33. Akagi, J. & Baba, H. Hydrogen gas restores exhausted CD8+ T cells in patients with advanced colorectal cancer to improve prognosis. *Oncol. Rep.* **41** (1), 301–311. <https://doi.org/10.3892/or.2018.6841> (2019).
34. Shinbo, T. et al. Breathing nitric oxide plus hydrogen gas reduces ischemia-reperfusion injury and Nitrotyrosine production in murine heart. *Am. J. Physiol. Heart Circ. Physiol.* **305** (4), H542–H550. <https://doi.org/10.1152/ajpheart.00844.2012> (2013).
35. Nishimura, N. et al. Pectin and high-amylose maize starch increase caecal hydrogen production and relieve hepatic ischaemia-reperfusion injury in rats. *Br. J. Nutr.* **107** (4), 485–492. <https://doi.org/10.1017/S0007114511003229> (2012).
36. Ishida, Y., Hino, S., Morita, T., Ikeda, S. & Nishimura, N. Hydrogen produced in rat colon improves *in vivo* reduction-oxidation balance due to induced regeneration of α -tocopherol. *Br. J. Nutr.* **123** (5), 537–544. <https://doi.org/10.1017/S0007114519003118> (2020).
37. Zhai, X. et al. Lactulose ameliorates cerebral ischemia-reperfusion injury in rats by inducing hydrogen by activating Nrf2 expression. *Free Radic Biol. Med.* **65**, 731–741 (2013).
38. Meyer, M., Tebbe, U. & Piiper, J. Solubility of inert gases in dog blood and skeletal muscle. *Pflügers Arch.* **Mar384** (2), 131–134. <https://doi.org/10.1007/BF00584428> (1980).
39. Liu, C. et al. Correction: corrigendum: Estimation of the hydrogen concentration in rat tissue using an airtight tube following the administration of hydrogen via various routes. *Sci. Rep.* **5**, 9629. <https://doi.org/10.1038/srep09629> (2015).
40. Zhang, X. et al. Molecular hydrogen inhibits colorectal cancer growth via the AKT/SCD1 signaling pathway. *Biomed. Res. Int.* **2022** (8024452). <https://doi.org/10.1155/2022/8024452> (2022).
41. Meng, X. et al. Hydrogen therapy reverses cancer-associated fibroblasts phenotypes and remodels stromal microenvironment to stimulate systematic anti-tumor immunity. *Adv. Sci. (Weinh)*. **11** (28), e2401269. <https://doi.org/10.1002/adv.202401269> (2024).
42. Hirano, S. I. et al. Molecular hydrogen as a novel antitumor agent: possible mechanisms underlying gene expression. *Int. J. Mol. Sci.* **22** (16), 8724. <https://doi.org/10.3390/ijms22168724> (2021).

43. Yan, H. et al. Microbial hydrogen manufactory for enhanced gas therapy and self-activated immunotherapy via reduced immune escape. *J. Nanobiotechnol.* **20** (1), 280. <https://doi.org/10.1186/s12951-022-01440-7> (2022).
44. Akagi, J. & Baba, H. Hydrogen gas activates coenzyme Q10 to restore exhausted CD8⁺ T cells, especially PD-1⁺Tim3⁺terminal CD8⁺ T cells, leading to better nivolumab outcomes in patients with lung cancer. *Oncol. Lett.* **20** (5), 258. <https://doi.org/10.3892/ol.2020.12121> (2020).
45. Ge, L. et al. Microbial hydrogen economy alleviates colitis by reprogramming colonocyte metabolism and reinforcing intestinal barrier. *Gut Microbes.* **14** (1), 2013764. <https://doi.org/10.1080/19490976.2021.2013764> (2022).
46. Zhang, C. B., Tang, Y. C., Xu, X. J., Guo, S. X. & Wang, H. Z. Hydrogen gas inhalation protects against liver ischemia/reperfusion injury by activating the NF- κ B signaling pathway. *Exp. Ther. Med.* **9** (6), 2114–2120. <https://doi.org/10.3892/etm.2015.2385> (2015).
47. Liu, X. et al. Hydrogen coadministration slows the development of COPD-like lung disease in a cigarette smoke-induced rat model. *Int. J. Chron. Obstruct Pulmon Dis.* **12**, 1309–1324. <https://doi.org/10.2147/COPD.S124547> (2017).
48. Shi, J. et al. Hydrogen saline is protective for acute lung ischaemia/reperfusion injuries in rats. *Heart Lung Circ.* **21** (9), 556–563. <https://doi.org/10.1016/j.hlc.2012.05.782> (2012).
49. Tanaka, Y., Xiao, L. & Miwa, N. Hydrogen-rich bath with nano-sized bubbles improves antioxidant capacity based on oxygen radical absorbing and inflammation levels in human serum. *Med. Gas Res.* **12** (3), 91–99. <https://doi.org/10.4103/2045-9912.330692> (2022).
50. Ishibashi, T. et al. Consumption of water containing a high concentration of molecular hydrogen reduces oxidative stress and disease activity in patients with rheumatoid arthritis: an open-label pilot study. *Med. Gas Res.* **2** (1), 27. <https://doi.org/10.1186/2045-9912-2-27> (2012).
51. Aoki, C. et al. Molecular hydrogen has a positive impact on pregnancy maintenance through enhancement of mitochondrial function and Immunomodulatory effects on T cells. *Life Sci.* **308**, 120955. <https://doi.org/10.1016/j.lfs.2022.120955> (2022).
52. Noda, K. et al. Hydrogen-supplemented drinking water protects cardiac allografts from inflammation-associated deterioration. *Transpl. Int.* **25** (12), 1213–1222. <https://doi.org/10.1111/j.1432-2277.2012.01542.x> (2012).
53. Kierkels, G. J. J. et al. Identification of a tumor-specific allo-HLA-restricted $\gamma\delta$ TCR. *Blood Adv.* **3**(19):2870–2882. (2019). <https://doi.org/10.1182/bloodadvances.2019032409>
54. Uldrich, A. et al. CD1d-lipid antigen recognition by the $\Gamma\delta$ TCR. *Nat. Immunol.* **14**, 1137–1145. <https://doi.org/10.1038/ni.2713> (2013).
55. Deseke, M. & Prinz, I. Ligand recognition by the $\Gamma\delta$ TCR and discrimination between homeostasis and stress conditions. *Cell. Mol. Immunol.* **17**, 914–924. <https://doi.org/10.1038/s41423-020-0503-y> (2020).
56. Wu, Z. et al. CD3+CD4-CD8- (Double-Negative) T cells in inflammation, immune disorders and cancer. *Front. Immunol.* **13**, 816005. <https://doi.org/10.3389/fimmu.2022.816005> (2022).
57. Aune, T. M., Collins, P. L., Collier, S. P., Henderson, M. A. & Chang, S. Epigenetic activation and Silencing of the gene that encodes IFN- γ . *Front. Immunol.* **4** (112), 16. <https://doi.org/10.3389/fimmu.2013> (2013).
58. de Araújo-Souza, P. S., Hanschke, S. C. & Viola, J. P. Epigenetic control of interferon-gamma expression in CD8 T cells. *J Immunol Res.* :849573. (2015). <https://doi.org/10.1155/2015/849573> (2015).
59. Sobue, S. et al. Molecular hydrogen modulates gene expression via histone modification and induces the mitochondrial unfolded protein response. *Biochem. Biophys. Res. Commun.* **4** (1), 318–324. <https://doi.org/10.1016/j.bbrc.2017.09.024> (2017).
60. Al-Qadami, G. H., Secombe, K. R., Subramania, C. B., Wardill, H. R. & Bowen, J. M. Gut Microbiota-Derived Short-Chain Fatty Acids: Impact on Cancer Treatment Response and Toxicities. *Microorganisms*. **10**(10): (2048). <https://doi.org/10.3390/microorganisms10102048> (2022).
61. Luu, M. et al. Microbial short-chain fatty acids modulate CD8⁺ T cell responses and improve adoptive immunotherapy for cancer. *Nat. Commun.* **12** (1), 4077. <https://doi.org/10.1038/s41467-021-24331-1> (2021).
62. Campbell, A. et al. H₂ generated by fermentation in the human gut Microbiome influences metabolism and competitive fitness of gut butyrate producers. *Microbiome* **11** (133). <https://doi.org/10.1186/s40168-023-01565-3> (2023).
63. Routy, B. et al. Melanoma and microbiota: current Understanding and future directions. *Cancer Cell.* **42** (1), 16–34. <https://doi.org/10.1016/j.ccell.2023.12.003> (2024).
64. Coutzac, C. et al. Systemic short chain fatty acids limit antitumor effect of CTLA-4 Blockade in hosts with cancer. *Nat. Commun.* **11**, 2168. <https://doi.org/10.1038/s41467-020-16079-2> (2020).
65. Uribe-Herranz, M. et al. Gut microbiota modulate dendritic cell antigen presentation and radiotherapy-induced antitumor immune response. *J. Clin. Invest.* **130** (1), 466–479. <https://doi.org/10.1172/JCI124332> (2020).
66. Hu, Y. et al. $\gamma\delta$ T cells: origin and fate, subsets, diseases and immunotherapy. *Signal. Transduct. Target. Ther.* **8** (1), 434. <https://doi.org/10.1038/s41392-023-01653-8> (2023).
67. Carabin, I. G. & Flamm, W. G. Evaluation of safety of inulin and oligofructose as dietary fiber. *Regul. Toxicol. Pharmacol.* **30** (3), 268–282. <https://doi.org/10.1006/rtp.1999.1349> (1999).
68. Cleverger, M. A. et al. Toxicological evaluation of Neosugar: genotoxicity, carcinogenicity, and chronic toxicity. *J. Am. Coll. Toxicol.* **7** (5), 643–662. <https://doi.org/10.3109/10915818809019540> (1988).
69. Cole, A. R. et al. Safety of inhaled hydrogen gas in healthy mice. *Med. Gas Res.* **9** (3), 133–138. <https://doi.org/10.4103/2045-9912.266988> (2019).
70. Salomez-Ihl, C. et al. Hydrogen inhalation: *in vivo* rat genotoxicity tests. *Mutat. Res. Genet. Toxicol. Environ. Mutagen.* **894**, 503736. <https://doi.org/10.1016/j.mrgentox.2024.503736> (2024).
71. Oliero, M. et al. Inulin impacts tumorigenesis promotion by colibactin-producing *Escherichia coli* in *ApcMin/+* mice. *Front. Microbiol.* **14**, 1067505. <https://doi.org/10.3389/fmicb.2023.1067505> (2023).
72. Yang, J. et al. High soluble fiber promotes colorectal tumorigenesis through modulating gut microbiota and metabolites in mice. *Gastroenterology* **166** (2), 323–337e7. <https://doi.org/10.1053/j.gastro.2023.10.012> (2024).
73. Asgharzadeh, F., Tarnava, A., Mostafapour, A., Khazaei, M. & LeBaron, T. W. Hydrogen-rich water exerts anti-tumor effects comparable to 5-fluorouracil in a colorectal cancer xenograft model. *World J. Gastrointest. Oncol.* **14** (1), 242–252. <https://doi.org/10.4251/wjgo.v14.i1.242> (2022).
74. Kajiya, M., Silva, M. J., Sato, K., Ouhara, K. & Kawai, T. Hydrogen mediates suppression of colon inflammation induced by dextran sodium sulfate. *Biochem. Biophys. Res. Commun.* **386** (1), 11–15. <https://doi.org/10.1016/j.bbrc.2009.05.117> (2009).
75. Chen, J. B. et al. Real world survey of hydrogen-controlled cancer: a follow-up report of 82 advanced cancer patients. *Med. Gas Res.* **9** (3), 115–121. <https://doi.org/10.4103/2045-9912.266985> (2019).
76. Salomez-Ihl, C. et al. H₂ inhalation therapy in patients with moderate COVID-19 (H₂COVID): a prospective ascending-dose phase I clinical trial. *Antimicrob. Agents Chemother.* **68** (8), e0057324. <https://doi.org/10.1128/aac.00573-24> (2024).
77. Gaboreau, Y. et al. Molecular hydrogen for outpatients with COVID-19 (Hydro-COVID): A phase 3 randomised, Triple-Blinded, pragmatic, Placebo-Controlled, multicentre trial. *J. Clin. Med.* **13** (15), 4308. <https://doi.org/10.3390/jcm13154308> (2024).
78. Hirano, S. I. & Takefuji, Y. Molecular hydrogen protects against various tissue injuries from side effects of anticancer drugs by reducing oxidative stress and inflammation. *Biomedicines* **12** (7), 1591. <https://doi.org/10.3390/biomedicines12071591> (2024).

Acknowledgements

The authors thank Sylvie Berthier (Cytometry Platform, CHUGA), Dr. Hervé Lerat and Maryline Cossin (PHTA Animal Facility). Orafit® GR inulin was generously donated by Beneo GmbH. This work was funded by Uni-

versité Grenoble-Alpes as part of the interdisciplinary program (CDTools) “My Health Companions” (MHC).

Author contributions

VPM contributed conceptualization, methodology, acquisition and analysis of the data and writing of the original draft. JPA contributed conceptualization, methodology, acquisition and analysis of the data and editing. ST and CSI contributed conceptualization, methodology and editing. PC contributed conceptualization, methodology, funding acquisition and editing. FB contributed conceptualization, methodology, acquisition and analysis of the data, writing of the original draft, funding acquisition and project administration. EB contributed conceptualization, methodology, acquisition and analysis of the data, writing of the original draft, funding acquisition and project administration.

Declarations

Competing interests

The authors declare no competing interests.

Additional information

Supplementary Information The online version contains supplementary material available at <https://doi.org/10.1038/s41598-025-96346-3>.

Correspondence and requests for materials should be addressed to F.B.

Reprints and permissions information is available at www.nature.com/reprints.

Publisher's note Springer Nature remains neutral with regard to jurisdictional claims in published maps and institutional affiliations.

Open Access This article is licensed under a Creative Commons Attribution-NonCommercial-NoDerivatives 4.0 International License, which permits any non-commercial use, sharing, distribution and reproduction in any medium or format, as long as you give appropriate credit to the original author(s) and the source, provide a link to the Creative Commons licence, and indicate if you modified the licensed material. You do not have permission under this licence to share adapted material derived from this article or parts of it. The images or other third party material in this article are included in the article's Creative Commons licence, unless indicated otherwise in a credit line to the material. If material is not included in the article's Creative Commons licence and your intended use is not permitted by statutory regulation or exceeds the permitted use, you will need to obtain permission directly from the copyright holder. To view a copy of this licence, visit <http://creativecommons.org/licenses/by-nc-nd/4.0/>.

© The Author(s) 2025